Growth of Hydroxyapatite crystals from solutions with pH controlled by novel vapor diffusion techniques. Effects of temperature and of the acidic phosphoprotein osteopontin on crystals growth

Roberto Mazzè

Secondary school with an emphasis on humanities "Giovanni Meli", Via Salvatore Aldisio, 2, 90146 Palermo, Italy
Former Faculty of Science - University of Palermo, Via Archirafi, 90123 Palermo, Italy

Abstract. — Crystals of hydroxyapatite were reproducibly grown utilizing 24-wells culture plates from aqueous metastable supersaturated calcium phosphate reacting solutions, under highly controlled conditions of pH and concentration of calcium and phosphate. Two novel growth techniques, based on diffusion of ammonia vapor produced by hydrolysis of ammonium phosphate, useful to buffer pH in the reacting solutions, were developed. Hydroxyapatite was grown from solutions, either at pH 7.4 without any acidic precursor in the temperature range 4 - 38 °C, or by the hydrolysis of brushite at 21, 38, 50 and 70 °C. The latter technique depends on raising the pH from 4.55 to 7.65, which causes the formation of octacalcium phosphate (pH ~ 5.5) as intermediate phase.

Subsequently theeffectsoftheacidicphosphoprotein osteopontin on crystals growth were studied carrying out additional sets of experiments, under identical conditions at 21 °C. When initially dispersed into the calcium phosphate mother solutions, osteopontin assumed a pivotal role to control nucleation and growth of brushite, octacalcium phosphate and hydroxyapatite. Moreover osteopontin slowed down kinetics of the phase transformations: brushite → octacalcium phosphate and octacalcium phosphate → hydroxyapatite.

Riassunto. — Cristalli di Idrossiapatite sono stati cresciuti riproducibilmente utilizzando piastre da coltura cellulare a 24 pozzetti in soluzioni acquose soprassature metastabili di fosfato di calcio. Tali soluzioni sono state sottoposte a condizioni altamente controllatesiaper i valoridipHcheperleconcentrazioni in calcio e fosfato. Sono state sviluppate due tecniche innovative di accrescimento basate sulla diffusione di vapori di ammonio, prodotti dall'idrolisi del fosfato di ammonio, che permettono di tamponare il pH nelle soluzioni reagenti. L'idrossiapatite è stata prodotta in soluzioni a pressione atmosferica sia per precipitazione diretta a pH 7,4 senza la comparsa di precursori acidi nell'intervallo di temperatura 4 - 38 °C che per idrolisi di brushite a 21, 38, 50 e 70 °C. Quest'ultima tecnica si basa sul graduale e controllato aumento del valore del pH da 4,55 a 7,65 che causa la formazione di ottocalciofosfato (pH ~ 5,5) come fase intermedia.

Successivamente sono stati studiati gli effetti della proteina acida osteopontina sulla crescita dei cristalli effettuando in condizioni identiche serie addizionali di esperimenti a 21 °C. Quando inizialmente dispersa nelle soluzioni originarie di fosfato di calcio, l'osteopontina assume un ruolo di cardinale importanza nel controllo della nucleazione e della crescita di brushite, ottocalciofosfato e idrossiapatite.

Per di più l'osteopontina rallenta le cinetiche delle trasformazioni di fase: brushite → ottocalciofosfato e ottocalciofosfato → idrossiapatite.

Key words: *Crystal growth, Brushite, Octacalcium phosphate, Hydroxyapatite, Hydrolysis, Phase transformations, acidic phosphoprotein, Osteopontin effects*

Introduction

Hydroxyapatite (HAP) is the inorganic phase most similar to the biological apatite (Betts *et al.*, 1981; Montel *et al.*, 1981; Newesely, 1989) which is the principal constituent of bones and teeth of vertebrates. HAP is frequently found within the pathological calcifications, like renal calculi (Santos and González-Díaz, 1980; Grases *et al.*, 1996), often associated with other calcium phosphates. The production of HAP arouses today a great interest because of its use as biocompatible osseous-integrating material (Tanahashi *et al.*, 1996; Hing *et al.*, 1997), eventually associated with metallic bio-inert substrate (De Groot *et al.*, 1987; Lemons, 1988; Wang *et al.*, 1997; Nonami *et al.*, 1998) (mainly titanium).

Over the last decennia, many authors proposed preparation methods to produce synthetic HAP (Boskey and Posner, 1976; Jarcho *et al.*, 1976; Nelson and Featherstone, 1982; Young and Holcomb, 1982; Abbona and Franchini-Angela, 1995; Kandori *et al.*, 1995; Lazić, 1995; Liu, 1995; Luo and Nieh, 1996). It is well known that HAP crystallizes according to the derivative $P6_3/m$ hexagonal space symmetry (Kay *et al.*, 1964) out of an array which, in its most ordered state, assumes a $P2_1/b$ monoclinic pseudo - hexagonal organization (Elliot *et al.*, 1973; Suda *et al.*, 1995).

The transformation of one acidic calcium phosphate like brushite (Monma and Kamiya, 1987; Fulmer and Brown, 1998) or octacalcium phosphate (OCP) (Cheng, 1987; Graham and Brown, 1996) was also utilized to produce HAP. Particularly, OCP is regarded as a transition product towards HAP formation, providing a template at physiological temperature and pH. The interactions between OCP and HAP were investigated by many researchers, that proposed epitactical (Nelson and McLean, 1984; Iijima *et al.*, 1996) or topotactical (Iijima *et al.*, 1997) mechanisms, due to the structural similarity of the two crystal structures along the direction [100].

The aim of this paper was the development of two techniques to produce with high reproducibility, from controlled solutions, synthetic HAP crystals, either at pH 7.4 without any acidic precursor (Mazzè and Deganello, 2000), or by the hydrolysis of brushite (Mazzè, 2002 c). The latter technique provides for the intermediate growth of OCP, which is the direct HAP acidic precursor. Consequently, because of the slow and controlled increase of pH from 4.55 to 7.65, the phase transformations brushite → OCP and OCP → HAP occurred. I believe that it is useful to have comparative terms compositionally similar to the biological apatitic material, to study either the normal and pathological mineralizations or the diagenetic processes, which concern the phosphatic remains during their burial (Mazzè, 2000; 2002 a; 2003 a).

Once tested the extreme experimental reproducibility in both growth techniques, other sets of experiments were carried out to determine if osteopontin (OPN) (Yoon *et al.*, 1987; Noda *et al.*, 1990; Chang and Prince, 1991; Craig and Denhardt, 1991), initially dispersed into the reacting solutions, could inhibit or promote the production of the involved crystals and consequently the kinetics of the two phase transformations (Mazzè, 2002 b). These studies were carried out because the substances able to promote or to inhibit the production of HAP *in vitro* could execute the same functions *in vivo*. In the mammalians bodies OPN is one of the principal acidic phosphoproteins found in cartilages, bones and dentine (Reinholt *et al.*, 1990; Denhardt and Guo, 1993), where it interacts both with the inorganic fraction and with the others proteins (Mckee and Nanci, 1996). Moreover it treats an intricate role in the control of bio-mineralizations (Hoyer, 1994; Mckee *et al.*, 1995; Min *et al.*, 1998) and it inhibits the nucleation and growth of HAP *in vitro* (Boskey *et al.*, 1993; Hunter *et al.*, 1996).

Materials and Methods

Crystal growth techniques

Work solutions were prepared from analytical grade reagents (Sigma-Aldrich; Merck), using

double distilled water further filtered (Millipore 0.22 μm).

Crystals were grown in the inner wells of 24-wells culture plates (Fig. 1) (Falcon #3047; 6 X 4 wells configuration).

At the beginning of each experiment metastable supersaturated calcium phosphate solutions were introduced into the inner four or eight wells of the culture plates according to diversified geometries; in addition, solutions of ammonium phosphate at pre-arranged concentration and pH were pipetted into each of the remaining wells surrounding the periphery of the plates. Finally the plates were isolated by the outside tightly sealing their covers with three layers of electrical tape, so that ammonia vapor, produced by hydrolysis of ammonium phosphate, diffused from the perimetrical into the central wells. Such a vapor diffusion regulated pH into the calcium phosphate solutions.

Since the plates were closed, the pH of the solutions was measured only at 21 °C for up to 340 hours connecting a recording-potentiometer (diameter 3 mm) to an electrode, which was introduced into one of the crystallization wells through a vapor – tight valve, adapted to a predrilled orifice in the sealing cover. pH was also monitored during each experiment directly by visual comparison with standard indicators (Merck #9531, #9533), which were placed into some crystallization wells. These plastic strips, which were suitably shortened to 2 cm, did not chemically contaminate the solution in the well, and permitted the pH to be monitored through the transparent cover, also when the crystallization systems were not disturbed for almost two years.

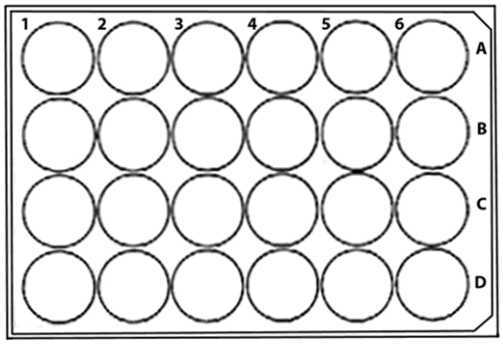

Fig. 1 – the 24-wells culture plate (6 X 4 well configuration)

Each kind of experiment was tested for reproducibility at least in quadruplicate after obtaining the optimal conditions of growth; furthermore, it was carried out many other times in order to have a large quantity of specimens to analyze.

Crystal growth technique 1. Growth of hydroxyapatite crystals at pH 7.4

The calcium phosphate reacting solution was prepared mixing 25 ml of calcium nitrate (0.28 M; pH 7.4 with NH_4OH 1:100) with 25 ml of a mixture of monobasic and dibasic ammonium phosphate (0.24 M; pH 7.4). After the initial precipitation of amorphous material the solution was filtered (Whatmann 20 – 25 μm) and its pH adjusted from 4.55 to 7.4 with 2.2 ml of Tris-TAM buffer 1M. The new amorphous material, precipitated because of such pH increase, was totally removed filtering the solution again (sequentially Whatmann filters 20 – 25 μm and 2.5 μm). 2 ml of such solution ([Ca] = 4.3 mM, [P] = 3.2 mM) were introduced into each of the eight central wells B2, B3, B4, B5, C2, C3, C4 and C5 of the culture plate. In addition, 2 ml of a mixture of monobasic and dibasic ammonium phosphate (0.5M, pH 7.3) were pipetted into each of the surrounding sixteen wells (A1, A2, A3, A4, A5, A6, B1, B6, C1, C6, D1, D2, D3, D4, D5 and D6). Finally the plate was closed sealing its cover with electrical type. Such isolation allowed vapor of ammonia, produced by hydrolysis within the sixteen perimetrical wells, to diffuse into the calcium phosphate reacting solutions, stabilizing their pH at 7.4. The experiment was carried out in the temperature range 4 (± 1) - 38 (± 0.5) °C.

Crystal growth technique 2. Growth of hydroxyapatite crystals by the hydrolysis of brushite

Initially the two lateral columns of wells A1, B1, C1, D1 and A6, B6, C6, D6, respectively at the far left and at the far right edges of the plates, were each covered with three layers of electrical type and were not used. The calcium phosphate reacting solution was prepared mixing 15 ml of calcium nitrate (0.28 M; pH 7.4 with NH_4OH 1:100) with 15 ml of a mixture of monobasic and dibasic ammonium phosphate (0.24 M; pH 7.4).

The initial precipitation of amorphous material was removed again filtering the solution (sequentially Whatmann filters: twice 20 – 25 µm and once 8 µm and 2.5 µm).

1.5 ml of such solution (pH 4.55; [Ca] = 55 mM, [P] = 40 mM) were introduced into each of the inner four central wells (B3, B4, C3 e C4) of the culture plate. In addition, 2 ml of a mixture of monobasic and dibasic ammonium phosphate (1M, pH 7.4) were pipetted into each of the surrounding twelve wells (A2, A3, A4, A5, B2, B5, C2, C5, D2, D3, D4 and D5) lining the periphery of the remaining part of the plate. As usual the plate was closed with electrical type. At 21 °C, in 74 hours enough ammonia diffused from the solutions within A2, A3, A4, A5, B2, B5, C2, C5, D2, D3, D4 and D5 into those within B3, B4, C3 and C4 in order to slowly raise their pH to 7.4. In these latter solutions within 54 hours pH reached the value of 5.5 and within 210 hours the value of 7.65, which was maintained for the duration of the experiment (Fig. 2). On the other hand the calcium concentration within 54 hours decreased from 55 mM to 16 mM; within 113 hours it reached the value of 1.5 mM and within 167 hours the value of 0.4 mM (Fig. 3).

This experiment was carried out at 21 (± 0.5), 38 (± 0.5), 50 (± 0.5) and 70 (± 0.5) °C.

Growth of hydroxyapatite crystals from solutions with osteopontin initially dispersed into

Other sets of experiments were carried out to study the effects induced by OPN on the growth of the phosphatic crystals and on the transformation kinetics. These experiments were carried out under identical experimental conditions only at 21 (± 0.5) °C.

Purified and lyophilized OPN was solubilized in double distilled water using stearin, to avoid its possible denaturation. Then it was dispersed into the calcium phosphate reacting solutions before closing the plates with electrical type.

In the crystal growth technique 1, 2 ml of the reacting solution were introduced into each of the wells B2, B3, B4, B5, C2, C3, C4 and C5. Various aliquots of OPN were also introduced into B4, B5, C2, C3, C4 and C5. Nine OPN concentrations were tested. Consequently two culture plates needed for each set of experiments. OPN final concentrations were 4×10^{-5}, 4×10^{-4}, 0.002, 0.004, 0.04, 0.08, 0.2, 2 and 10 µg/ml. The two wells B2 and B3 always were the OPN – free controls. It was possible to carry out these experiments only in duplicate because I had not enough OPN, due to the difficulty of its purification.

In the crystal growth technique 2, 1.5 ml of the reacting solution were introduced into each of the wells B3, B4, C3 and C4. B3 was the OPN – free control. Various aliquots of OPN were also introduced into B4, C3 and C4 to obtain respectively the final concentrations 4.4×10^{-3}, 0.022 and 0.066 µg/ml. Such experiment was carried out in triplicate.

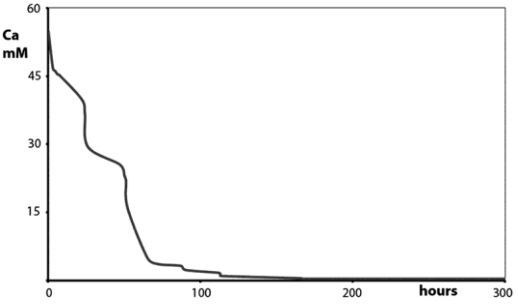

Fig. 3 – Reduction of the calcium concentration of the calcium phosphate reacting solution used for crystal growth technique 2 at 21 °C. To plot this curve were utilized the solutions of 24 crystallization baths since the experiments were broken off after fixed times.

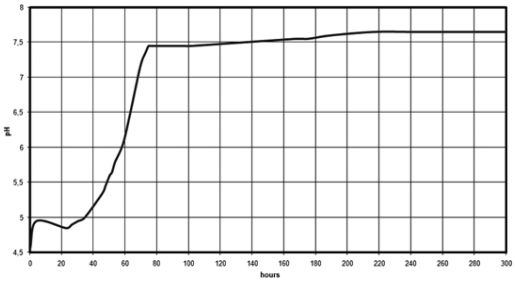

Fig. 2 - pH raise of the calcium phosphate reacting solution used for crystal growth technique 2 carried out at 21 °C. The curve was plotted monitoring the pH potentiometrically in triplicate.

Analytical techniques

Solutions and crystals were analyzed by atomic absorption spectroscopy, colorimetric arrays and HPLC (High Performance Liquid Chromatography).

Calcium concentration was determined by atomic absorption spectroscopy with a Perkin-Elmer 1100B using a wavelength line of 422.7 nm of an air - acetylene flame. The unknown solutions contained 5000 ppm of lanthanum to suppress phosphorus interference on calcium absorption. The same amount of lanthanum was put into each of four standard solutions covering the instrumental sensibility range. Each analysis was performed in quadruplicate.

Phosphate concentration was determined as the blue phosphomolybdenum complex with a Perkin Elmer 55B equipped with a red filter using a wavelength line of 880 nm. Ascorbic acid was selectively used to reduce the molybdenumphosphoric acid. Six phosphate solutions, containing weighed aliquots of standard (KH_2PO_4), were prepared to construct the calibration curve. Absorbance for standard and unknown solutions was taken against a blank reagent, exactly 30 minutes after the color developed.

Calcium and phosphorus were also measured by ionic chromatography with a self regenerating suppressor (HPLC, Dionex 2000SP. Anions: column Ion Pac AS4A - SC, 1.3 ml/min. Cations: column Ion Pac S12A, 1.2 ml/min).

The Ca/P ratio of the crystals was determined dissolving aliquots in 100 µl cold ultra-pure nitric acid using a Pyrex depression slide. These solutions were aspired with an Hamilton syringe and each of them diluted into 25 milliliters of double distilled water. Once in solution, calcium and phosphorus were respectively measured by atomic absorption spectroscopy and colorimetrically as described above.

Optical And electron Microscopy

The processes of nucleation, growth and hydrolysis were continuously monitored with a stereomicroscope operating with transmitted and reflected light. The morphology of the crystals was examined by an Axiomat microscope (plane and polarized light) as well as by scanning electron microscopy (SEM) using two Cambridge instruments (Stereoscan 360; LEO 430) operating at 15 kV and at 80 – 300 pA. To carry out such observations the plates were opened at fixed times quenching the experiment. Crystals were accurately aspirated out from the solutions using micro - pipettes, then they were washed three times with double distilled water, air dried under a nitrogen jet and gently harvested.

In order to do SEM observations the dried crystals were mounted on aluminum stubs, using a silver-based conductive cement or a double adhesive carbon type, and finally they were coated with gold or carbon by under vacuum glow discharge.

X-ray diffraction

X-ray diffraction patterns were taken from crystals exclusively using a Gandolfi camera (114.6 mm) and Ni-filtered radiation (35 – 40 kV; 15 – 20 mA) operating under vacuum (3×10^{-2} torr). Such analyses were extensively tested for each crystallization bath.

X-ray diffraction patterns were also taken from the initial amorphous material (Ni – filtered Cu Kα; 40 kV, 20 mA, $2\theta = 1°$/min; Cps 200, 400, 1000).

The unambiguous identifications of the phases were done using A.S.T.M. Fiche Numbers 11-293 and 9-432 as references respectively for brushite and HAP. The X-ray diffraction patterns were also calculated with Powder Cell analysis program (W. Kraus and G. Nolze, BAM, Berlin) so that OCP was also identified. These calculations contributed to index the diffraction peaks.

The lattice constants were obtained by the least square method using 2θ values of at least fourteen diffraction peaks from 30 to 70 degrees, and silicon as internal standard only for crystals growth at 21 °C.

Modelling of the atomic structures was done with the program ATOMS (ESM Software, Inc., Cincinnati, OH, USA) using, like for the diffraction patterns calculations, the atomic coordinates and the lattice cell parameters of Curry and Jones (1971) and Abbona *et al.* (1994) for brushite, of

Mathew *et al.* (1988) for OCP, of Kay *et al.* (1964) and Sudarsanan and Young (1969) for HAP.

MicroAnAlyses

Simultaneously with SEM observations micro - chemical EDS analyses (Oxford-Link 5431; ZAF correction program; counting time 100 – 200 s) were routinely carried out operating at 15 kV. Ca and P were the only analyzed elements. When possible other parts of the same samples exposed to X-ray were used.

Thin - polished sections, approximately 40 μm thick, were prepared for five groups of cogenetic HAP crystals grown at pH 7.4, that were allowed to remain in solution respectively for 8, 21, 48, 390 and 600 days. Then nine to thirty-two micro-chemical quantitative spot analyses per sample were carried out using a Cameca - Camebax electron microprobe, operating at 15 kV and 15 nA in the WDS mode for a total of 96 WDS analyses. Counting times were 10 s at the peak and 10 s at the background. These examination physical conditions were a compromise to obtain suitable analytical precision and to minimize destructive effects due to the electronic bombardment. Analyses were performed against a synthetic standard apatite. X-ray counts were converted into oxide weight as well as atomic percentages using the PAP correction program (Pouchou, 1984). These analyses are typically precise to within 1% for major elements.

Results

The two crystal growth techniques here presented were optimized after lots of attempts altering the concentrations of the initial calcium and phosphate work solutions as well as the analytical reagents.

Both techniques were highly reproducible at all tested temperature. The kinetics of nucleation, growth and hydrolysis processes were proportionally slowed or accelerated respectively at lower and higher temperatures.

Crystal growth technique 1

HAP grew as crystals (size apparent values 5 x 4 x 0.2 μm) aggregated to form hemispheric concretions (diameter apparent values ~ 150 μm) (Fig. 4). Any morphological variation was observed

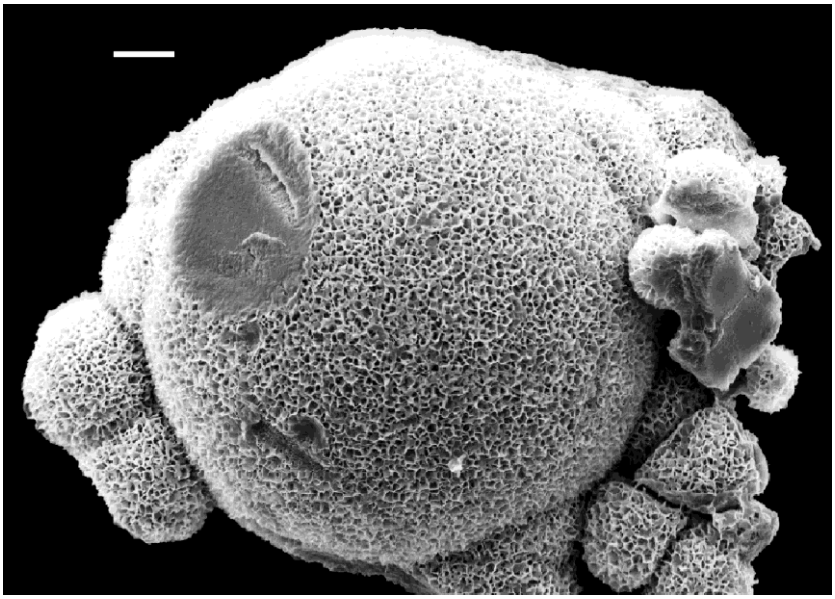

Fig. 4 – Scanning electron micrograph of hemispheric concretions of HAP grown by means of technique 1. The bar: 20 μm.

in the HAP crystals as a function of temperature which was maintained stable for the duration of each experiment.

X-ray (Fig. 5) and microprobe WDS analyses demonstrated that the concretions were exclusively formed by HAP. In each X-ray analysis effects of diffraction due to other phases or to modifications of the spatial group were not detected. Crystals were stable within the mother solutions also when the experiments were extended more than two years. Along this time pH was stable at 7.4. The kinetics of nucleation and growth were regulated only by the temperature; the concretions were microscopically observed after 8, 24 and 157 hours respectively at 38, 21 and 4 °C.

The structural order of the crystals was good starting from the first stages of growth. When crystals were allowed to remain nine months within the mother solution, such order was particularly emphasized by the correct intensities and by the good resolution of the diffraction peaks 100, 200, 002, 211, 112, 300, 202, 310, 222, 312, 213, 321, 410, 402, 004, 411, 151, 511.

The Ca/P ratios were calculated using the atomic percentages measured in the WDS mode from every data point (Table 1). Such ratios were variable between the limit values of 1.45 as minimum and 1.76 as maximum. This variation is attributable to order – disorder phenomena (Boskey and Posner, 1976; Betts *et al.*, 1981; Montel *et al.*, 1981; Nelson and Featherstone, 1982; Gadaleta *et al.*, 1996) because of the exclusively hydroxyapatitic diffraction patterns of the crystals.

Crystal growth technique 2

At 21 °C crystals of brushite rapidly nucleated and grew in few minutes just next to the liquid - vapor interface at the top of the metastable calcium phosphate solutions. Their growth was complete after approximately 40 hours since the plates were closed (typical mean size apparent values 200 x 120 x 10 µm) (Fig. 6). Fig. 7(a) shows their high quality x-ray diffraction pattern. These clear and colorless crystals were always tiny and flat with the characteristic tabular habitus. They were usually elongated according to the [001]'s or to the [101]'s. The {010}'s was the dominant and well developed crystal form. Simple and multiple twins as well as polycrystalline aggregates were common crystallization products. The lattice constants (SG = *Ia*) were **a** = 5.825(5) Å, **b** = 15.199(12) Å, **c** = 6.249(4) Å, **β** = 116°49,4'(0,54). Some crystal generations were observed. Crystals with smaller

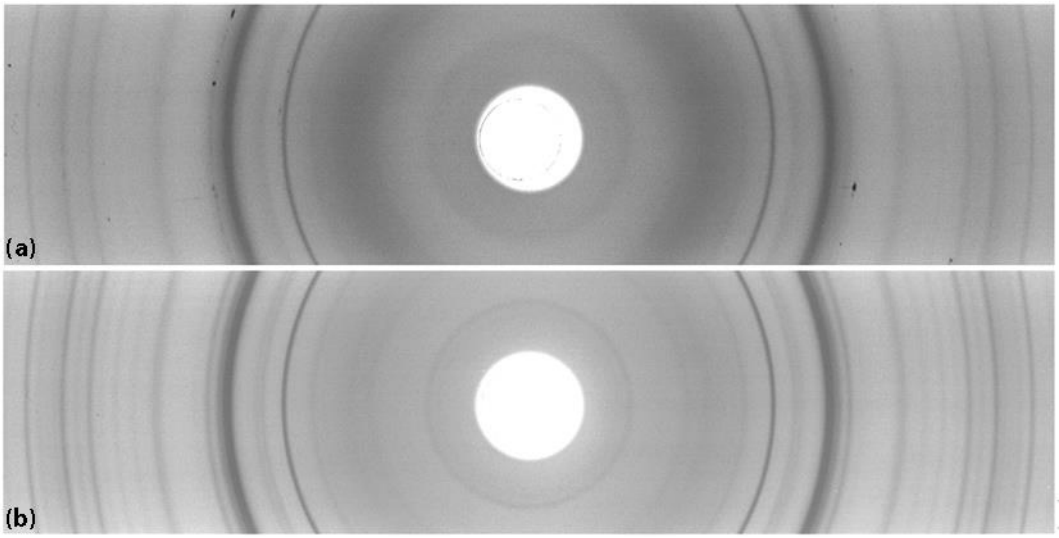

Fig. 5 – X-ray diffraction patterns taken from HAP crystals grown by means of technique 1. Crystals were allowed to remain respectively 8 days (a) and 9 months (b) within their mother solutions.

table 1
Microchemical quantitative spot analyses carried out in the WDS mode for HAP crystals grown by means of technique 1.

8 days	W%(O)	W%(P)	W%(Ca)	W% tot	A%(O)	A%(P)	A%(Ca)	Tot A%	Ca/P
1	32.59	15.54	31.37	79.50	61.33	15.10	23.57	100	1.56
2	32.07	15.25	31.00	78.31	61.29	15.06	23.65	100	1.57
3	32.43	15.52	31.03	78.98	61.38	15.18	23.44	100	1.54
4	32.82	15.66	31.55	80.03	61.34	15.12	23.54	100	1.56
5	31.05	14.54	30.75	76.34	61.08	14.77	24.15	100	1.63
6	31.45	14.86	30.71	77.03	61.20	14.94	23.86	100	1.60
7	32.01	15.27	30.79	78.08	61.34	15.11	23.55	100	1.56
8	32.40	15.50	31.05	78.95	61.37	15.16	23.47	100	1.55
9	29.62	13.88	29.31	72.81	61.09	14.78	24.13	100	1.63
10	34.11	16.68	31.49	82.27	61.69	15.58	22.73	100	1.46
11	33.33	16.21	31.04	80.58	61.61	15.48	22.91	100	1.48
12	29.98	13.94	30.03	73.96	60.98	14.64	24.38	100	1.67
13	33.63	16.35	31.37	81.35	61.60	15.47	22.93	100	1.48
14	32.26	15.36	31.10	78.72	61.31	15.09	23.60	100	1.56
15	33.95	16.47	31.75	82.16	61.58	15.44	22.99	100	1.49

21 days	W%(O)	W%(P)	W%(Ca)	W% tot	A%(O)	A%(P)	A%(Ca)	Tot A%	Ca/P
1	29.13	13.95	27.86	70.93	61.39	15.18	23.43	100	1.54
2	33.04	15.92	31.29	80.25	61.47	15.29	23.24	100	1.52
3	35.15	17.21	32.38	84.74	61.70	15.61	22.69	100	1.45
4	33.09	15.98	31.19	80.26	61.51	15.35	23.14	100	1.51
5	34.89	16.81	33.00	84.70	61.48	15.30	23.22	100	1.52
6	35.21	17.09	32.92	85.21	61.58	15.44	22.98	100	1.49
7	35.37	17.14	33.17	85.68	61.55	15.40	23.04	100	1.50
8	33.84	16.40	31.74	81.97	61.55	15.40	23.04	100	1.50
9	35.62	17.36	33.07	86.05	61.64	15.52	22.84	100	1.47

dimension, corresponding to lower supersaturation values, had also the best habitus with plane, straight and well developed faces.

In time, pH gradually raised reaching the value of 7.65 because of the ammonia vapor diffusion from the outer to the four central wells. When after 54 hours pH reached the value of approximately 5.5 (Fig.2) OCP, which was the stable phase (Monma and Kamiya, 1987), began to nucleate and grow at the expense of brushite crystals. OCP grew as prismatic hexagonal single crystals (size apparent values 10 x 5 x 0.6 μm) aggregated to form spherulites (Fig. 8). Fig.3 shows the reduction in the calcium concentration which underwent a drastic decrement again after 54 hours when the first nuclei of OCP formed and began to growth.

Table 1
Continued...

48 days	W%(O)	W%(P)	W%(Ca)	W% tot	A%(O)	A%(P)	A%(Ca)	Tot A%	Ca/P
1	37.66	18.30	35.14	91.10	61.60	15.46	22.94	100	1.48
2	37.08	17.97	34.74	89.79	61.56	15.41	23.02	100	1.49
3	38.45	18.72	35.75	92.93	61.63	15.50	22.87	100	1.48
4	38.48	18.67	36.02	93.18	61.57	15.43	23.01	100	1.49
5	38.11	18.54	35.52	92.17	61.61	15.48	22.92	100	1.48
6	37.28	18.19	34.55	90.02	61.65	15.54	22.81	100	1.47
7	37.37	18.18	34.79	90.34	61.61	15.49	22.90	100	1.48
8	37.20	18.18	34.38	89.76	61.68	15.57	22.75	100	1.46
9	38.30	18.45	36.25	93.00	61.47	15.30	23.23	100	1.52
10	38.09	18.57	35.36	92.02	61.64	15.52	22.84	100	1.47
11	35.09	16.82	33.49	85.41	61.40	15.20	23.39	100	1.54
12	35.08	16.58	34.24	85.90	61.21	14.94	23.85	100	1.60
13	35.52	16.91	34.27	86.71	61.31	15.08	23.61	100	1.57
14	34.66	16.53	33.37	84.56	61.33	15.10	23.57	100	1.56
15	34.63	16.32	33.96	84.91	61.17	14.89	23.95	100	1.61
16	34.57	16.32	33.82	84.72	61.19	14.92	23.90	100	1.60
17	35.35	16.74	34.39	86.48	61.24	14.98	23.78	100	1.59
18	32.48	15.23	32.09	79.80	61.10	14.80	24.10	100	1.63
19	38.59	18.72	36.13	93.44	61.57	15.42	23.01	100	1.49
20	38.34	18.72	35.49	92.55	61.66	15.55	22.79	100	1.47
21	36.44	17.32	35.28	89.04	61.28	15.04	23.68	100	1.57
22	35.62	16.85	34.72	87.20	61.22	14.96	23.82	100	1.59
23	36.68	17.57	35.05	89.30	61.39	15.19	23.42	100	1.54
24	33.35	15.57	33.18	82.11	61.04	14.72	24.24	100	1.65
25	35.41	16.97	33.83	86.21	61.40	15.19	23.41	100	1.54
26	37.42	18.12	35.12	90.67	61.55	15.39	23.06	100	1.50
27	31.24	14.46	31.48	77.19	60.93	14.57	24.51	100	1.68
28	31.21	14.34	31.77	77.32	60.83	14.44	24.72	100	1.71
29	31.89	14.51	32.95	79.35	60.70	14.26	25.04	100	1.76
30	31.02	14.34	31.33	76.69	60.91	14.54	24.55	100	1.69
31	35.07	16.30	35.11	86.49	60.98	14.64	24.37	100	1.66
32	32.09	14.59	33.17	79.85	60.69	14.26	25.05	100	1.76

Table 1
Continued...

13 months	W%(O)	W%(P)	W%(Ca)	W% tot	A%(O)	A%(P)	A%(Ca)	Tot A%	Ca/P
1	38.37	18.63	35.84	92.84	61.59	15.45	22.96	100	1.49
2	38.74	18.73	36.47	93.94	61.52	15.36	23.12	100	1.50
3	38.74	18.76	36.34	93.84	61.55	15.40	23.05	100	1.50
4	36.78	17.44	35.73	89.96	61.25	15.00	23.75	100	1.58
5	37.75	18.11	35.99	91.84	61.41	15.22	23.37	100	1.54
6	36.72	17.61	35.02	89.36	61.41	15.21	23.38	100	1.54
7	36.81	17.57	35.40	89.78	61.34	15.12	23.54	100	1.56
8	37.87	18.23	35.89	91.99	61.46	15.29	23.25	100	1.52
9	36.58	17.23	35.91	89.71	61.16	14.88	23.97	100	1.61
10	37.26	17.77	35.86	90.89	61.33	15.11	23.56	100	1.56
11	36.52	17.31	35.47	89.31	61.25	15.00	23.75	100	1.58
12	36.77	17.48	35.57	89.82	61.29	15.05	23.67	100	1.57
13	35.75	16.99	34.59	87.33	61.28	15.05	23.67	100	1.57

Fig. 9 shows the coexistence of some growing OCP spherulites over the (010) face of one dissolving brushite crystal. Under stereoscopic microscopy the progressive dissolution of the brushite crystals appeared complete after about two weeks. On the contrary, in this stage, their traces were revealed by X-ray analyses (Fig. 7b). At the final value reached by pH (7.65) HAP was the stable phase that slowly formed to the expenses of the OCP crystallites.

During the progressive formation of HAP no growth of new aggregates of crystals was noticed. This let me hypothesize that HAP genesis was not a random but an *in situ* phenomenon, controlled by the atomic transforming structure of OCP. On the other side, such transformation was gradual as underlined by the diffraction patterns. In such patterns the gradual disappearance of the OCP diffraction peaks was observed concomitantly to the appearance and the increase of intensity of the hydroxyapatitic ones. X-ray data showed that, in the final products, OCP, recognizable by the very weak diffraction peaks 100 (d = 18.632 Å), $1\bar{1}0$ (d = 9.385 Å) and 010 (d = 9.019 Å), was dispersed in a well crystallized hydroxyapatitic matrix. In the final stadium, under SEM, HAP crystals appeared morphologically irregular, unlike the previous OCP ones (Fig. 10). The high structural order of HAP was particularly suggested by the right intensities and by the good resolution of the diffraction peaks 100, 200, 002, 211, 112, 300, 202, 310, 222, 312, 213, 321, 410, 402, 004, 411, 151, 511. The lattice parameters **a** = 9.434(5) Å and **c** = 6.884(3) Å were calculated from crystals remained in solution 16 months.

The OCP → HAP transformation was also monitored by the Ca/P ratios that provided the measure of the relative presence of the two phases within the crystallization products. Ca/P values were 1.39, 1.47 and 1.59 respectively after 14, 36 and 300 days of growth. Since Ca/P ideal ratio of stoichiometric OCP is 1.33, data suggest a very weak presence of HAP after 14 days of growth (Table 2).

Systematically SEM observations, EDS and X-ray analyses were carried out from crystals that were allowed to grow for 42 hours, 8, 13, 23 and 33 days at 38, 50 and 70 °C.

At 38 °C very weak traces of brushite were only recognized in the diffraction pattern taken from crystals that were allowed to continue hydrolyzing for a total of 42 hours (Fig. 11a). Such pattern

Table 1
Continued...

20 months	W%(O)	W%(P)	W%(Ca)	W% tot	A%(O)	A%(P)	A%(Ca)	Tot A%	Ca/P
1	36.79	17.47	35.66	89.93	61.27	15.03	23.71	100	1.58
2	38.23	18.52	35.85	92.60	61.55	15.40	23.05	100	1.50
3	38.60	18.74	36.09	93.43	61.58	15.44	22.98	100	1.49
4	38.91	18.76	36.77	94.44	61.49	15.32	23.20	100	1.51
5	38.65	18.72	36.27	93.63	61.55	15.40	23.06	100	1.50
6	38.46	18.60	36.19	93.26	61.53	15.37	23.11	100	1.50
7	38.70	18.70	36.47	93.86	61.51	15.35	23.14	100	1.51
8	35.94	16.98	35.11	88.03	61.20	14.93	23.87	100	1.60
9	38.03	18.32	36.01	92.35	61.47	15.29	23.24	100	1.52
10	36.56	17.35	35.47	89.38	61.26	15.01	23.73	100	1.58
11	37.56	17.71	36.81	92.07	61.17	14.90	23.93	100	1.61
12	38.30	18.36	36.53	93.20	61.41	15.21	23.38	100	1.54
13	35.27	16.61	34.63	86.51	61.16	14.87	23.97	100	1.61
14	39.23	18.92	37.09	95.24	61.48	15.31	23.20	100	1.52
15	35.99	16.86	35.64	88.49	61.08	14.78	24.14	100	1.63
16	36.96	17.46	36.12	90.55	61.20	14.93	23.87	100	1.60
17	37.25	17.61	36.36	91.23	61.21	14.94	23.85	100	1.60
18	36.86	17.22	36.65	90.73	61.05	14.73	24.23	100	1.64
19	38.60	18.36	37.28	94.24	61.30	15.07	23.64	100	1.57
20	36.06	16.76	36.13	88.94	60.98	14.64	24.39	100	1.67
21	35.74	16.83	35.09	87.67	61.16	14.88	23.97	100	1.61
22	34.98	16.31	34.86	86.15	61.02	14.70	24.28	100	1.65
23	39.24	18.80	37.50	95.54	61.39	15.19	23.42	100	1.54
24	35.96	16.77	35.84	88.57	61.02	14.70	24.28	100	1.65
25	37.26	17.50	36.73	91.49	61.12	14.83	24.05	100	1.62
26	36.13	16.79	36.18	89.10	60.98	14.64	24.38	100	1.67
27	36.16	16.81	36.22	89.19	60.98	14.64	24.38	100	1.67

shows that the hydrolysis products were almost entirely constituted by OCP, as any hydroxyapatitic diffraction peak was not recognized. HAP was positively identified after 8 days and 42 hours of growth respectively at 38 °C (Fig. 11) and 50 °C (Fig. 12). At this last temperature brushite was never revealed by X-ray analyses.

At these temperatures the transformation OCP → HAP was almost total respectively after 23 (38 °C) and 8 days (50 °C). Such a transformation was total after 42 hours at 70 °C. Fig. 13 shows the morphological degrade of the crystals that occurred during the transformation. Particularly Fig. 13 (a) shows OCP Crystals, (b) and (d) OCP

transforming into HAP, (c) HAP crystals with weakly X-ray traces of OCP. Crystals formed at 50 and 38 °C, appeared under similar morphological conditions respectively after 42 hours and 13 days of growth.

Osteopontin effects on crystals growth

These sets of experiments were carried out only at 21 °C because at this temperature the phase transformations are opportunely slowed down and to study also the protein – brushite crystals interaction.

In crystal growth technique 1 nucleation and growth of HAP were totally inhibited starting by 0.08 µg/ml OPN. In this case any precipitation of crystals was not observed for the duration of the experiment (20 months). On the contrary both the nucleation and the growth of HAP were considerably delayed starting by concentration of 4×10^{-4} µg/ml OPN and greater (0.04 µg/ml). Such a delay was not caused by 4×10^{-5} µg/ml OPN.

Instead 0.04 µg/ml OPN first delayed and after promoted the nucleation and the growth of HAP. Indeed, after the delay in their own growth, the self – aggregation of the crystals formed hemispheric concretions having final dimensions increased about 20 – 30 folds with respect to those growing in the OPN – free controls (Fig. 14).

In addition, OPN modulated the double transformation process. The hydrolysis of brushite was slowed down by OPN beginning from the concentration of 0.022 µg/ml (Fig. 15). Such concentration slowed down also the following transformation: OCP→HAP. These stabilizing effects were respectively corroborated by the diffraction patterns taken from powdered crystals exposed to 0.022 and 0.066 µg/ml OPN that were allowed to continue growing respectively for 17 days (Fig. 16) and 1 month (Fig. 17). Thus OPN stabilized first the brushite crystals and those of OCP then, favouring their permanence in solutions as metastable phases.

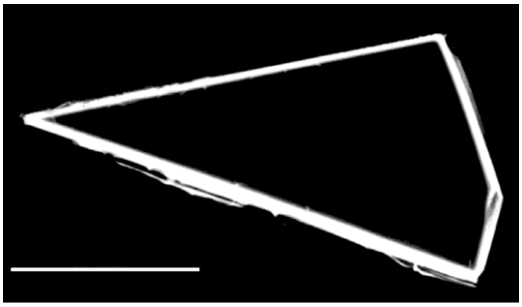

Fig. 6 – Scanning electron micrograph of a regular crystal of brushite grown at 21 °C. Note the well developed morphology of {010}. The bar: 50 µm.

Moreover such protein, even at lowest concentration tested (4.4×10^{-3} µg/ml), had also a debilitating effect on crystals morphology. Particularly, brushite crystals, grown in proximity of the wells top, lost the original habitus and showed a characteristic increase in the surface area of their {010}'s (Fig. 15). Such effects were best observed in the wells with higher OPN concentration.

discussion And Conclusion

Both the crystal growth techniques here presented start from mother solutions with concentrations higher than those utilized in literature to precipitate HAP (Boskey and Posner, 1976; Young and Holcomb, 1982; Abbona and Franchini-Angela,

table 2

Occurence and disappearance of brushite, OCP and HAP in the crystal growth technique 2 performed at 21 °C as function of pH values

	Brushite	**OCP**	**HAP**
pH	4.55	5.5	7.65
Occurence time	Few minutes	54 hours	336 hours
Total disappearance	After 336 hours	After 14 months	Stable phase

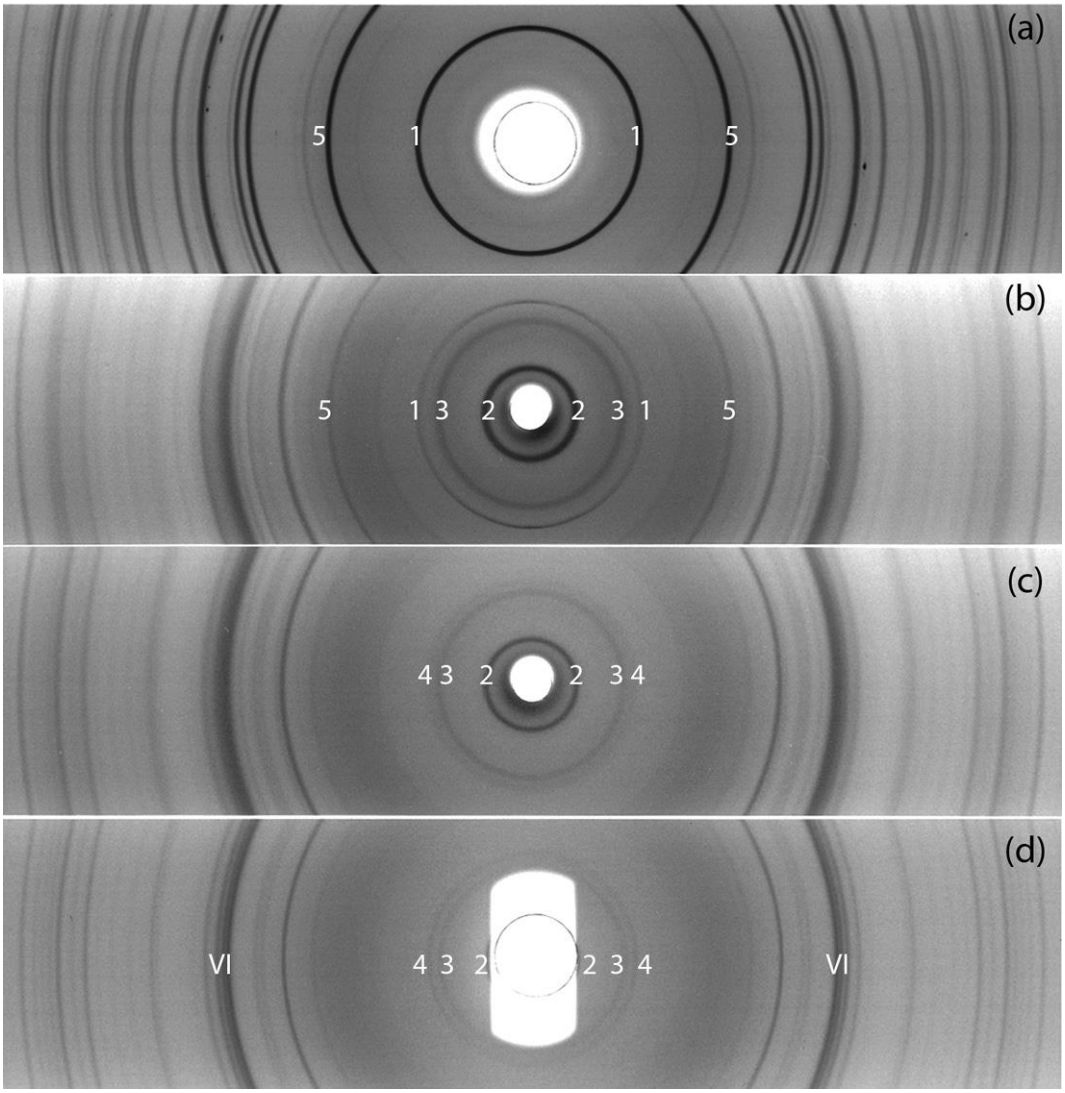

Fig. 7 – X-ray diffraction patterns taken from crystals grown at 21 °C by means of technique 2. Crystals were allowed to continue growing respectively for 24 hours (a), 14 days (b), 195 days (c), 14 months (d). (a) contains only the diffraction peaks of brushite, (b) also the OCP ones. In time, OCP diffraction peaks gradually disappeared concomitantly to the appearance and the increase of intensity of the HAP ones (c) and (d). Some diagnostic diffraction peaks are pointed out. Number1 020 (d = 7,59 Å; I/rel = 100) and number5 12-1 (d = 4,2367 Å; I/rel = 87,29) plus -121 (d = 4,2367 Å; I/rel = 86,52) of brushite; number2 100 (d = 18,6316 Å; I/rel = 100) and number3 1-10 (d = 9385 Å; I/rel = 16,70) plus 200 (d = 9,3158 Å; I/rel = 0,58) plus 010 (d = 9,0187 Å; I/rel = 18,36) of OCP; number4 100 (d = 8,1684 Å; I/rel = 7,87) and number VI respectively 211 (d = 2,8168 Å; I/rel = 100) plus 121 (d = 2,8168 Å; I/rel = 44,76), 112 (d = 2,7795 Å; I/rel = 71,69), 300 (d = 2,7228 Å; I/rel = 88,80) of HAP.

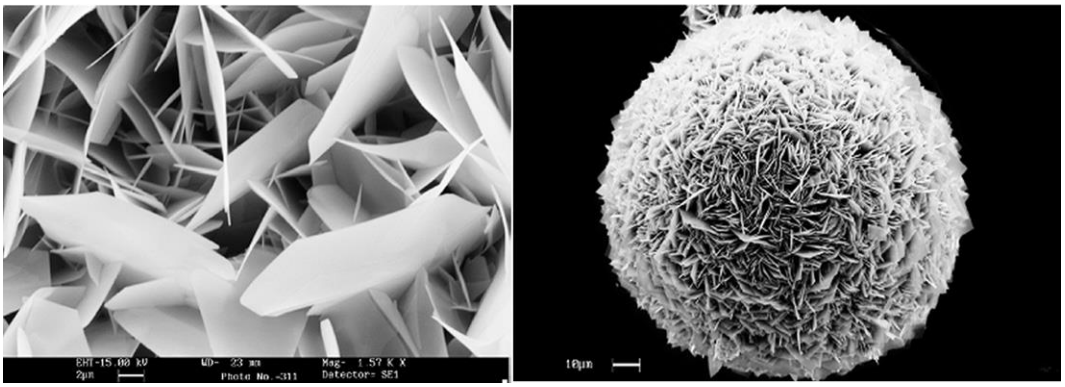

Fig. 8 – Scanning electron micrograph: OCP prismatic hexagonal single crystals (size apparent values 10 x 5 x 0.6 µm) aggregated to form spherulites.

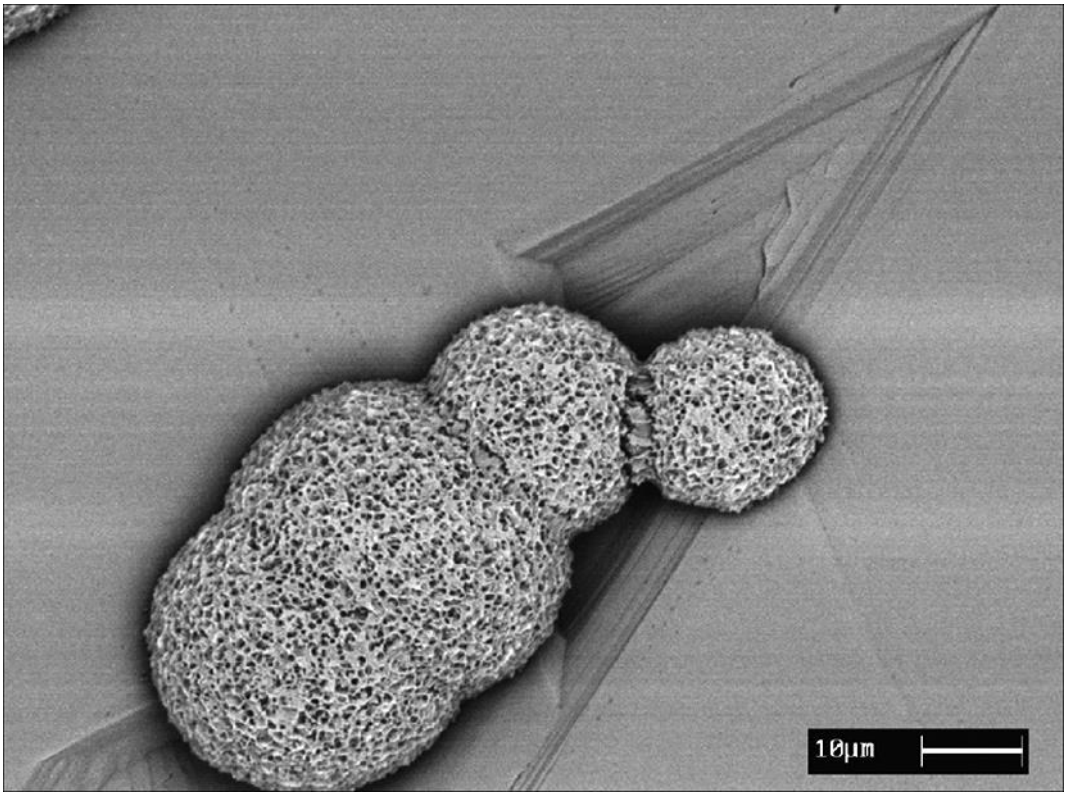

Fig. 9 – Scanning electron micrograph of OCP spherulites growing on the (010) face of a large tabular crystal of brushite in hydrolysis. Crystals were allowed to continue growing for 100 hours. Note the parallel exfoliation of the brushite crystal.

1995; Lazić, 1995; Liu, 1995; Luo and Nieh, 1996) so that at the end of the two processes is possible to obtain considerable quantities highly reproducibly of synthetic HAP crystals.

The preliminary steps, particularly in the case of crystal growth techniques 1, enable me to start the HAP crystallization processes from active and opportunely pH - buffered mother solutions. This

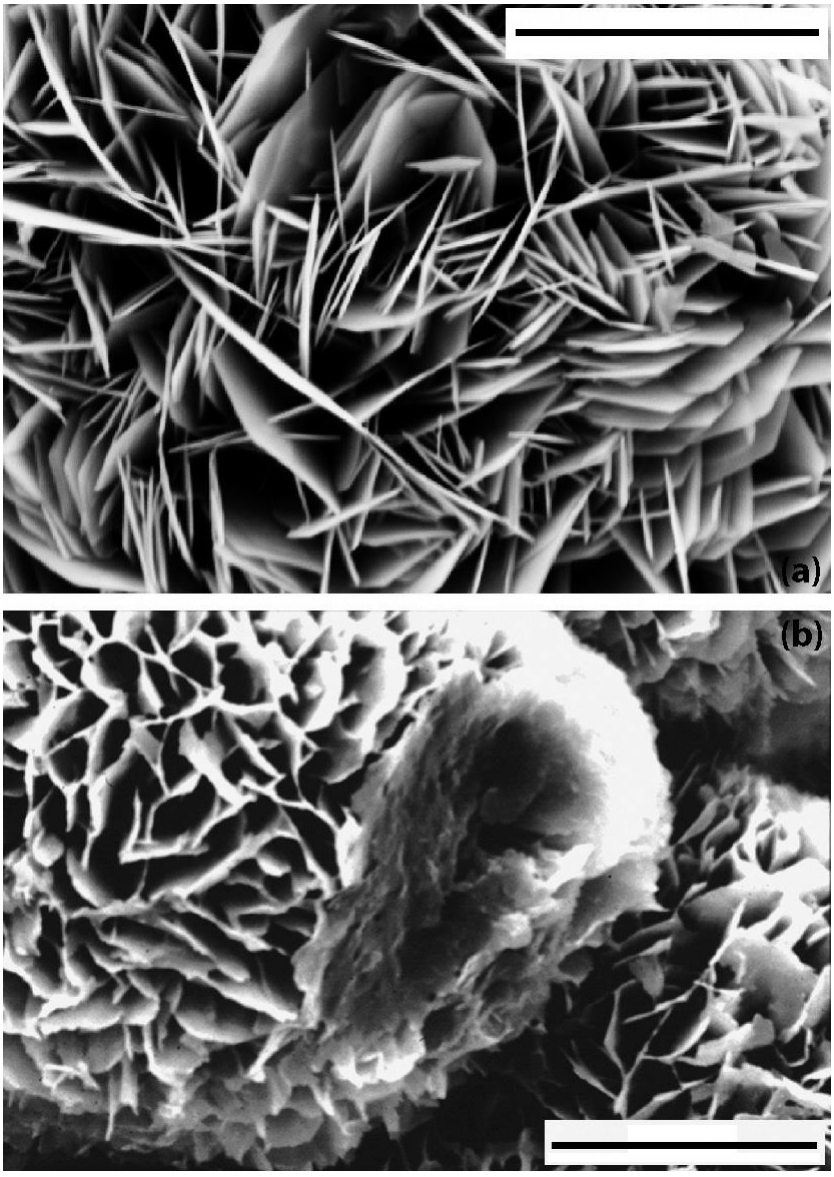

Fig. 10 – Scanning electron micrographs of OCP (a) and HAP (b) crystals which were allowed to continue growing respectively for 20 days and 14 months. Note the regular morphology of OCP crystals in opposition to the irregular one of HAP crystals. The bar: (a) 10 µm, (b) 20 µm.

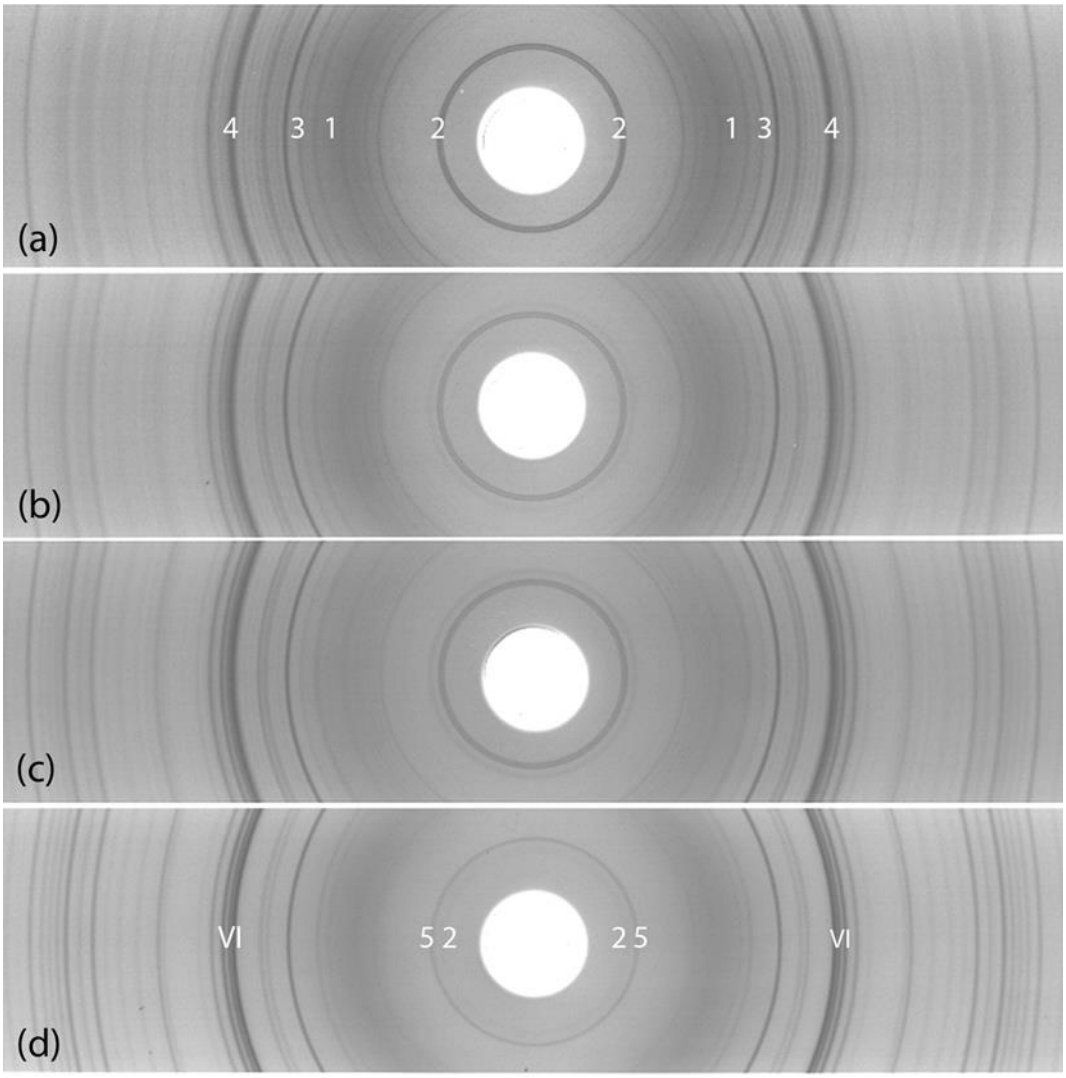

Fig. 11 – X-ray diffraction patterns taken from crystals grown at 38 °C by means of technique 2. Crystals were allowed to continue growing for 42 hours (a) and for 8 (b), 13 (c), 23 (d) days. Note that the transformations brushite → OCP and OCP → HAP were almost total respectively after 42 hours and 23 days. Some diagnostic diffraction peaks are pointed out. Number1 12-1 (d = 4,2367 Å; I/rel = 87,29) plus -121 (d = 4,2367 Å; I/rel = 86,52) very weak of brushite; number2 1-10 (d = 9385 Å; I/rel = 16,70) plus 200 (d = 9,3158 Å; I/rel = 0,58) plus 010 (d = 9,0187 Å; I/rel = 18,36), number3 3-21 (d = 3,6599 Å; I/rel = 39,18), number4 from 321 (d = 2,8523 Å; I/rel = 17,48) to 7-10 (d = 2,8094 Å; I/rel = 12,38) of OCP; number5 100 (d = 8,1684 Å; I/rel = 7,87) and number VI respectively 211 (d = 2,8168 Å; I/rel = 100) plus 121 (d = 2,8168 Å; I/rel = 44,76), 112 (d = 2,7795 Å; I/rel = 71,69), 300 (d = 2,7228 Å; I/rel = 88,80) of HAP.

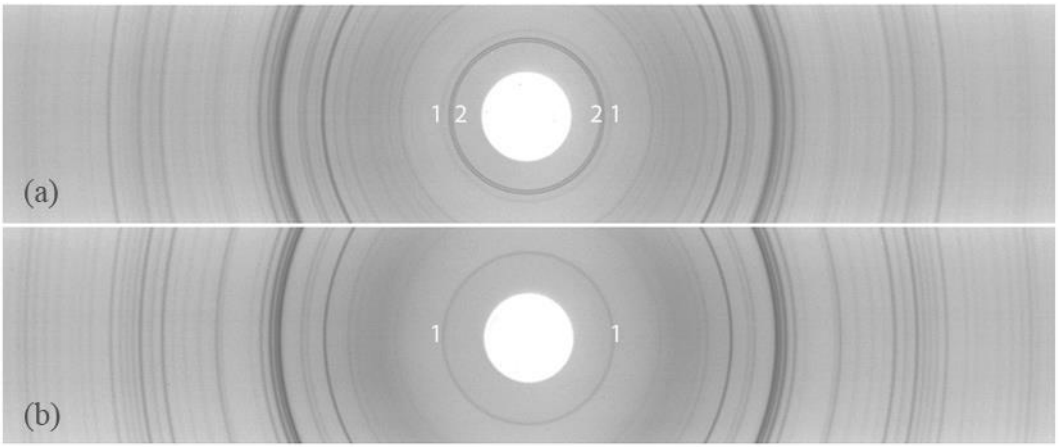

Fig. 12 – X-ray diffraction patterns taken from crystals grown at 50 °C by technique 2. Crystals were allowed to continue growing for 42 hours (a) and 8 days (b). Note that the transformation OCP → HAP was total after 8 days. Number1 point out 100 (d = 8,1684 Å; I/rel = 7,87) diffraction peak of HAP; number2 point out 1-10 (d = 9385 Å; I/rel = 16,70) plus 200 (d = 9,3158 Å; I/rel = 0,58) plus 010 (d = 9,0187 Å; I/rel = 18,36) diffraction peaks of OCP.

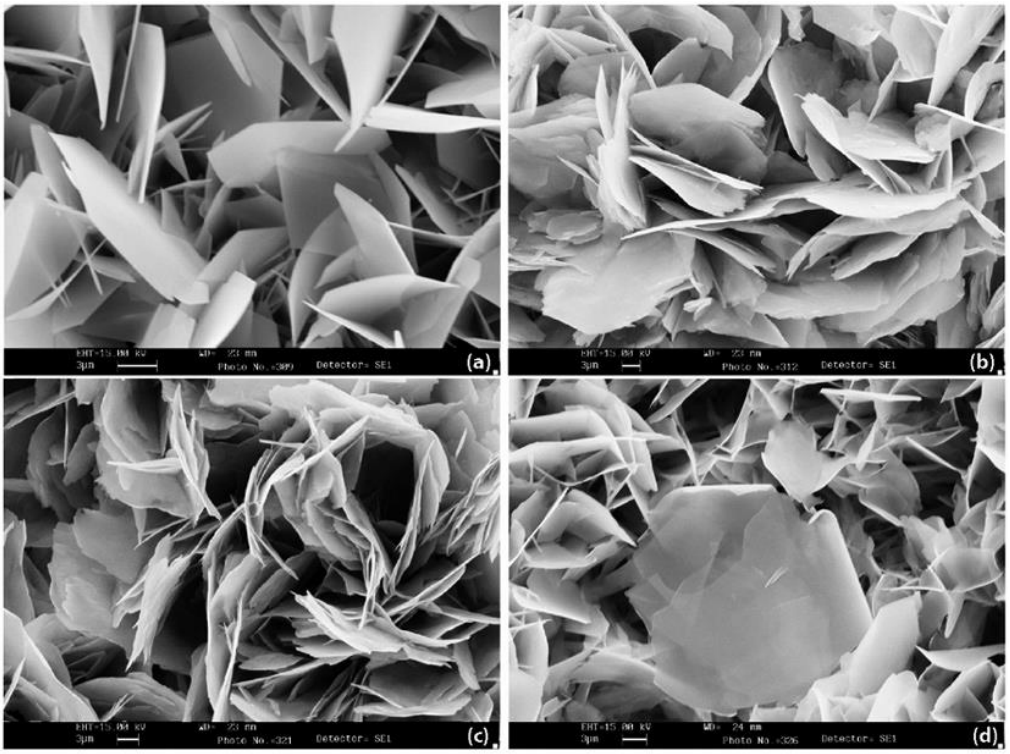

Fig. 13 – Scanning electron micrographs of crystals grown after the hydrolysis of brushite at 38 °C (a), (b), (c) and 50 °C (d). Crystals were allowed to continue growing for 42 hours (a), (d), and respectively for 13 (b) and 23 (c) days. (a) shows OCP Crystals, (b) and (d) OCP transforming into HAP, (c) HAP crystals with weakly X-ray traces of OCP. Note the faster morphological degrade of the crystals which occurred at 50 °C.

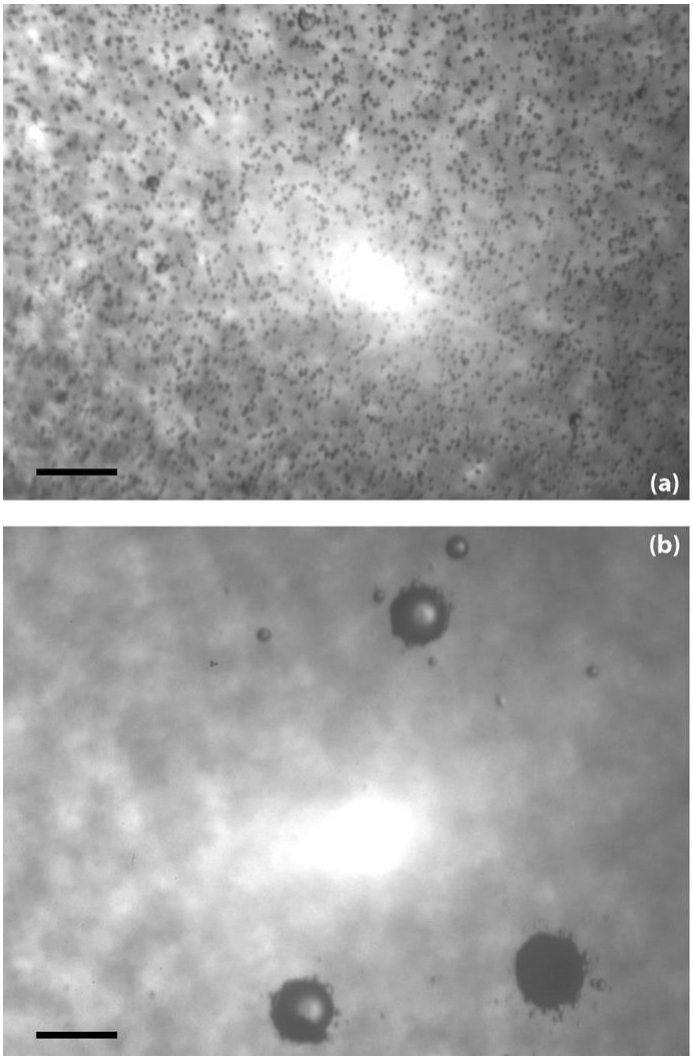

Fig. 14 – Spherulites of HAP grown by means of technique 2 respectively in presence of 4 x 10^{-4} µg/ml (a) and 0.04 µg/ml (b) OPN. Notice the increase in size of the hemispheric aggregates grown in presence of 0.04 µg/ml OPN. Bar 300 µm.

is not possible when one 4.3 mM calcium solution and one 3.2 mM phosphate solution are directly mixed because the precipitation of amorphous material anyway occurs owing to the high initial concentrations.

The Ca/P mother solutions ratio lower than the HAP stoichiometric one enable also to stabilize the acidic calcium phosphate precursors for a longer time in crystal growth technique 2 and shows the HAP crystals can directly growth from one active medium like the initial solutions of crystal growth technique 1 even to the detriment of ions concentrations if the pH value is correct.

The results indicated that when pH prevented HAP precipitation, both brushite and OCP could grow from solutions. If pH was to increase, such phases, during their own transformation, modulated the formation of HAP.

The hydrolysis process was reversible. Such a property was verified in the crystal growth technique 2 decreasing with ultrapure cloridric acid (30 %, 9.46 N) the pH of the crystallization baths from 7.65 to 4.55 at the end of the brushite → OCP and OCP → HAP phase transformations. So the anomalous recoveries of brushite in some bio - remains were potentially explained (Piepenbrink, 1989). This set of experiments will be presented in another work of mine actually in preparation concerning the diagenetic processes of the phosphatic remains during their burial.

Ammonium phosphate was employed as a source of ammonia vapor, which diffused over the

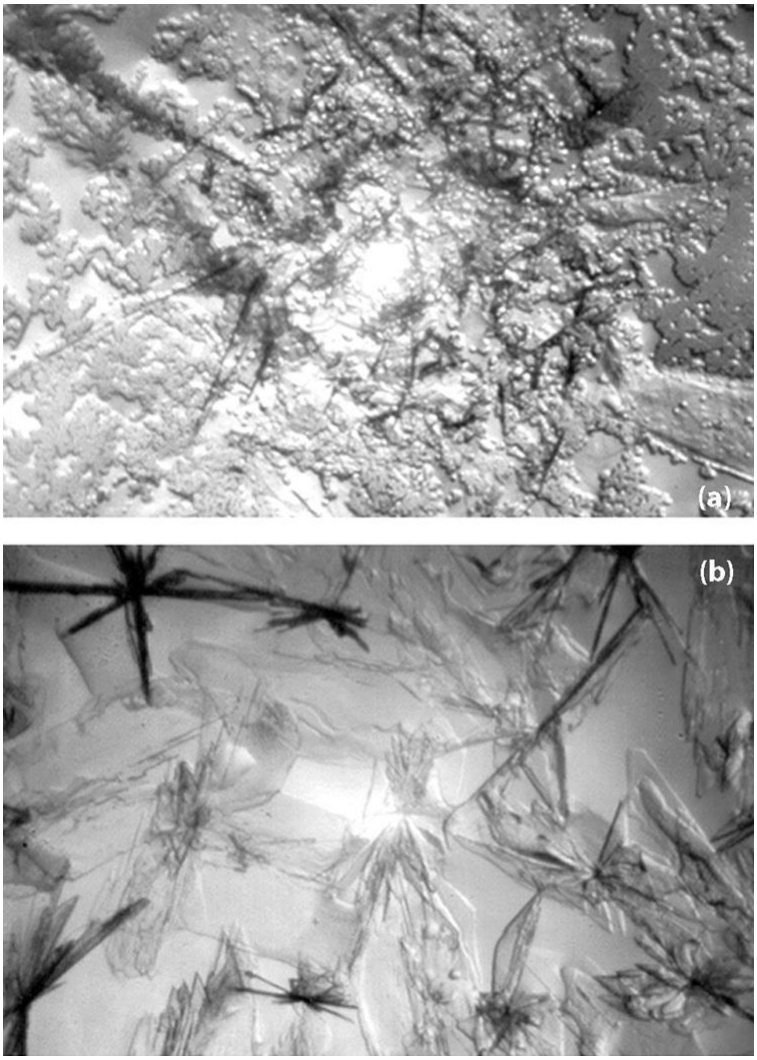

Fig. 15 – Crystals grown by means of technique 2 in absence (a) and in presence of 0.022 µg/ml (b) OPN which slowed the kinetic of the brushite → OCP phase change. (a) and (b) 20X. Note that OPN prevented the growth of OCP spherulites clearly visible in (a) and it caused the lost of the original habitus of the brushite crystals and the increase in the surface area of their {010}'s (b).

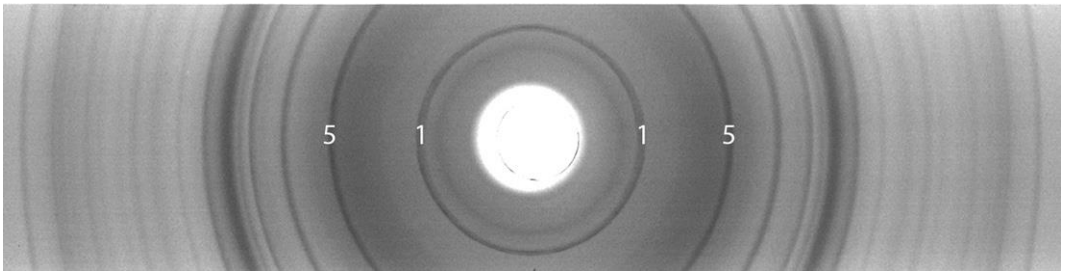

Fig. 16 – X-ray diffraction pattern taken from crystals grown in presence of 0.022 µg/ml OPN. Such crystals were allowed to continue growing for 17 days. Note the intensities of the brushitic diffraction peaks also in comparison with those of the diffraction patterns of Fig. 7. Some diagnostic diffraction peaks are pointed out identically to Fig. 7. Indeed number1 020 (d = 7,59 Å; I/rel = 100) and number5 12-1 (d = 4,2367 Å; I/rel = 87,29) plus -121 (d = 4,2367 Å; I/rel = 86,52) of brushite.

metastable calcium phosphate reacting solutions. So it was possible to minimize the variables inside the sealed plates. Moreover, as ammonia is far more volatile than phosphate to which it is initially complexed, it became an excellent stabilizer of the solutions pH in which crystals grew. Once again in solutions, ammonia, acting like base, took protons away from the reacting solutions, stabilizing their pH and contrasting with the antagonist dissociations of the phosphatic species and of the water, in the case of HAP growth. Such dissociations produced the anionic clusters that were immobilized in the crystal lattice of the growing phase, as the solutions were supersaturated. Furthermore, ammonium did not hinder phosphate uptake by calcium atoms.

The Ca/P atomic ratio of HAP crystals furnishes indications about the quantitative occupation of Ca sites (Betts *et al.*, 1981) and the potential substitution of $(PO_4)^{3-}$ with $(CO_3)^{2-}$ (Montel *et al.*, 1981; Nelson and Featherstone, 1982; Gadaleta

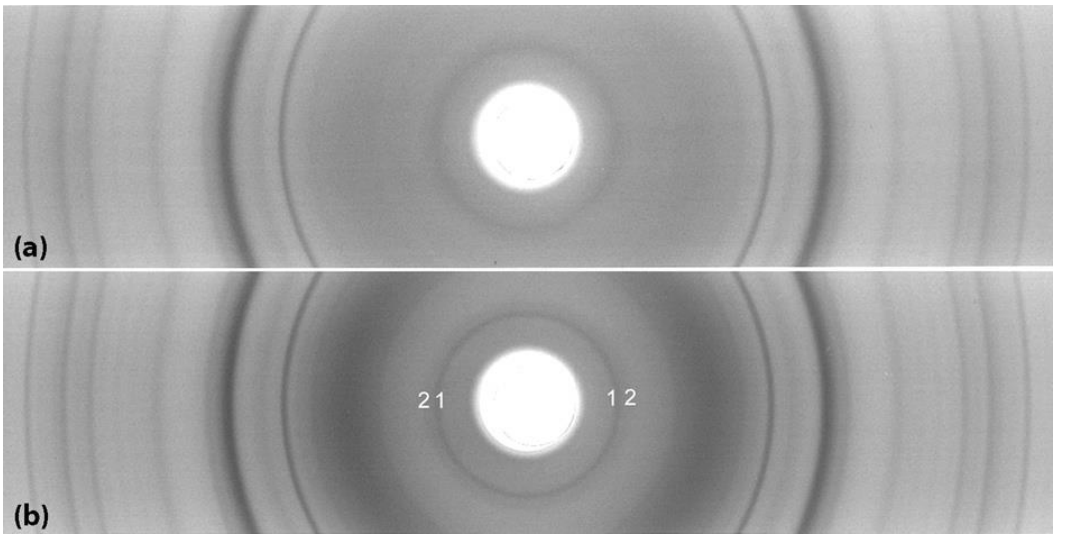

Fig. 17 – X-ray diffraction pattern taken from crystals grown in absence (a) and in presence of 0.066 µg/ml (b) OPN. Such crystals were allowed to continue growing for 1 month. Number 1points out 1-10 (d = 9,3850 Å; I/rel = 16,70), 200 (d = 9,3158 Å; I/rel = 0,58) and 010 (d = 9.0187 Å; I/rel = 18,36) OCP diffraction peaks; number 2 points out 100 (d = 8,1684 Å; I/rel = 7,87) HAP diffraction peak.

et al., 1996). Boskey and Posner (1976) proposed values varying from 1.60 to 1.73 as the direct consequence of Ca and P measures in the reacting solutions. Data from this work suggested that Ca/P ratios over 1.76 or under 1.45 do not appear structurally representative. Ca/P ideal ratio of a stoichiometric apatite, in absence of order - disorder phenomena, is 1.67. Crystal growth technique 2 proved that values under 1.45 were consistent with the presence of OCP (Ca/P = 1.33) within the crystals. Values over 1.76 would be presumably due to an extra - structural contribution of calcium. Calcite is a possible carrier which I produced in synthesis from solutions with excess of Ca^{2+} and $(CO_3)^{2-}$ ions (2003 b).

The hydrolysis of brushite crystals was particularly observed through their {010} form (Fig. 9). Structurally the (010) face is only composed of sets of hydrogen atoms and sets of oxygen atoms W(1) and W(2) (Fig. 18) from two crystallographically independent water molecules, having as y/b fractional coordinate respectively 0.0527(1) and 0.0739(1) (Abbona *et al.*, 1994). Besides, these atoms bound the d_{020} slices one to another by weak hydrogen bonds, notoriously constructing a layered and corrugated structure. These bonds were easily broken when crystals occurred as metastable in a less acidic medium, with the consequence that they parallely exfoliated to their {010}'s. In all probability crystals of brushite hydrolyzed themselves starting by W(1) and W(2) as well as by hydrogen atoms and sequentially involving the structurally contiguous atoms. Thus calcium and phosphate, once structurally bounded, were able to go into solutions again and then incorporated into the new forming OCP crystalline structure.

With regard to the OCP → HAP transformation data seem to suggest that the structural similarity of the two phases was critical. Particularly, a correspondence along the **c** axis exists between the Ca atoms, that in the HAP structure occupy the Ca(2) sites, and the Ca atoms, that in the OCP structure occupy the Ca(5), Ca(7) and Ca(6), Ca(8) sites. In such transformation the main event is the loss of the water molecules that, in the OCP structure, are placed along layers parallel to the **b** and **c** axes. Such loss is responsible of the characteristic structural collapse which, in this work, was observed through the morphological degrade of the HAP crystals, in opposition to the regular crystalline hexagonal habitus of the OCP crystals.

The crystal growth techniques, here discussed, are useful to provide suitable comparative correlations with the inorganic apatitic fraction of teeth and bones of the mammals (Mazzè, 2000; 2002 a; 2003 c).

Besides, data proved that osteopontin, when dispersed within the reacting solutions, drastically modulated nucleation and growth of brushite, OCP and HAP. Particularly, the interaction OPN – HAP happened both when crystals grew at pH 7.4 and when they formed through an acidic precursor. In these interactions the kinetic action prevailed over the thermodynamic equilibria.

With regard to the protein - brushite crystal interaction it seems that some specific polar parts of the OPN molecule selectively bonded themselves to the potential sites of the (010) faces, furnished by the extensive network of their superficial water molecules. Thus the (010) faces offered maximum resistance to hydrolysis destabilization. When OPN was free to interact with brushite it shielded the planes of the {010} form from the rest of the solution. Such action prevented the release of hydrogen, W(1), W(2) and of their structurally contiguous atoms into the mother solutions, so that the brushite hydrolysis and the new OCP crystals formation were delayed. Moreover, the adsorption of OPN was responsible for the debilitating morphological effects, due to the increase of the surface area of the {010} form.

When OPN was dispersed within the reacting solutions used for HAP crystals growth technique 1, the bulk of the process established highly selective specialized bonding interactions between Ca^{2+} ions and parts of its molecule. Ca^{2+} ions were subtracted from solutions so that the nucleation and growth of HAP crystals were totally inhibited, starting by 0.08 µg/ml OPN. At lower concentrations than the mentioned above, OPN stabilized HAP crystal nuclei lowering their energy of nucleation. Thus, their growth was favored and could continue undisturbed forming, at the concentration of 0.04 µg/ml of protein, greater hemispheric concretions with respect to those growing within the control wells (Fig. 14). Although one could exclude it *a priori*, such a process might be also controlled by selective bonding interactions that OPN

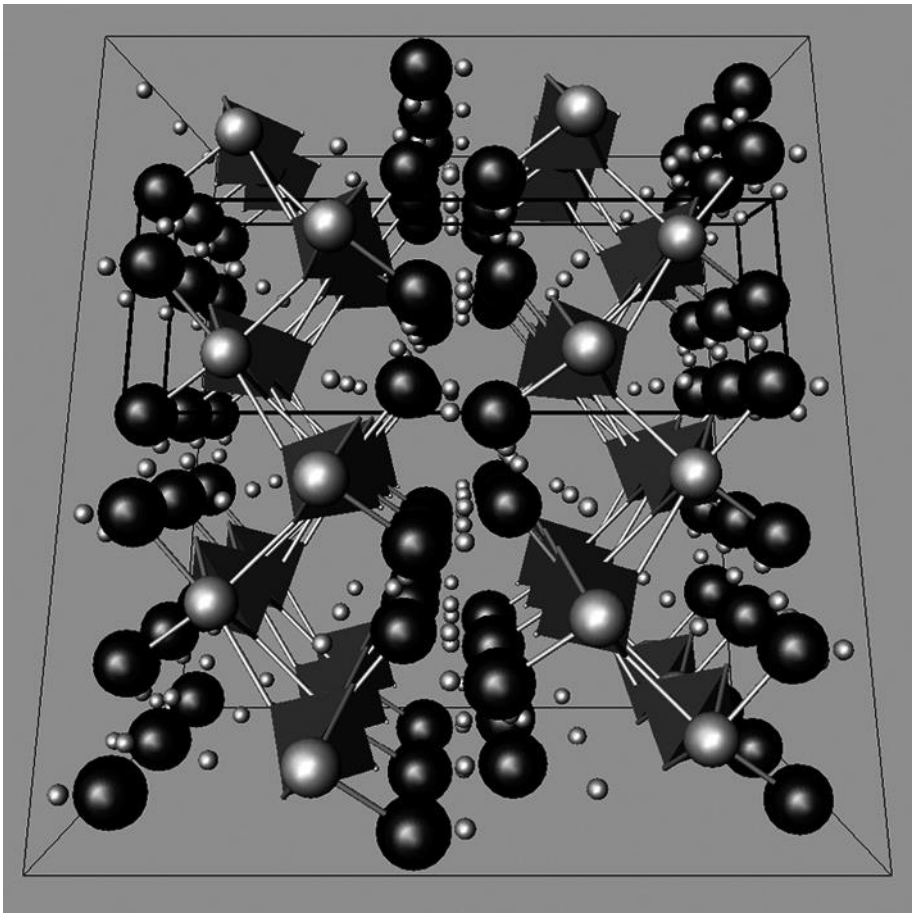

Fig. 18 – A schematic 3D projection along [001] of the brushite structure. Black circles: W(1) and W(2) oxygen atoms; great grey circles: calcium atoms; little grey circles: hydrogen atoms. The unit cell is underlined. (010) is the cleavage plane. Note that the (010) faces at the far left and at the far right edges of the three – dimensional figure are composed of sets of oxygen and hydrogen atoms. Those atoms are available both to start crystals hydrolysis and to furnish potential bonding sites to OPN when dispersed into the solutions.

establishes with Ca^{2+} ions in solution, and/or with some specific calcium sites on the HAP surface. It could seem probable that the calcium atoms subject to such specific action are those surfacing with respect to the {100} form and, to a greater degree, to the {001} one, due to its surface larger than the lateral hexagonal prism. Structurally the HAP (001) face is composed of a set of calcium atoms having almost zero height along ***c*** axis. In a manner similar of that described for the (010) faces of the brushite crystals, this crystallographical organization, unique to the (001), potentially provides an extensive network of bonding sites. These faces are not usually discriminated on HAP synthetic crystals grown under standard conditions (Boskey and Posner, 1976; Jarcho *et al.*, 1976; Nelson and Featherstone, 1982; Young and Holcomb, 1982; Abbona and Franchini-Angela, 1995; Kandori *et al.*, 1995; Lazić, 1995; Liu, 1995; Luo and Nieh, 1996) owing to their indefinite habitus. Nevertheless, many other studies are necessary to confirm such mechanism.

On the other hand the OPN quantity which totally inhibited the formation of HAP at pH 7.4 is lower than the medium physiological urinary concentration found in adult and healthy subjects (1.9 µg/ml) as the identical amino acid sequence of uropontin (Min *et al.*, 1998). The medium uropontin content found within renal hydroxyapatitic calculi is generally lower than 10 µg per 100 mg of calcification (Hoyer, 1994). In addition OPN is normally produced by many kinds of cells, it is found on a great variety of tissues and it is especially concentrated at the regions of the bone surface, and generally at the mineralization fronts and interfaces. In conclusion, osteopontin is certainly a particular protein able to prevent the pathological calcifications, as renal calculi. It is also able to play a pivotal role both in the formation and in the stabilization of normal mineralized tissues.

AcKnowledgeMents

I am grateful to G.I. Lampronti and A. Bigi for their helpful reviews and useful suggestions that improved the manuscript. Thanks are expressed to G. Molin for the assistance in the microprobe analyses. Osteopontin was kindly provided by F.G. Toback. I am also grateful to Luca Bindi for him impeccable editorial capacity.

REFERENCES

AbbonA f., cAlleri M., frAnchini-AngelA M. and ivAldi G. (1994) - *Synthetic brushite, $CaHPO_4 2H_2O$: Correct polarity and surface features of some complementary forms.* Neues Jahrb. Mineral. Abh. **168**, 171-184.

AbbonA F. and frAnchini-AngelA M. (1995) - *Crystallization of hydroxyapatite from very dilute solutions.* Neues Jahrb. Mineral. Monatsh., **12**, 563-575.

betts f., bluMenthAl N.C. and posner A.S. (1981) - *Bone mineralization.* J. Cryst. Growth, **53**, 63-73.

bosKey A.l., MArescA M., ullrich w., doty s.b., butler W.T. and prince C.W. (1993) - *Osteopontin – Hydroxyapatite interactions in vitro: inhibition of hydroxyapatite formation and growth in a gelatin gel.* Bone and Miner., **22**, 147-159.

bosKey A.L. and posner A.S. (1976) - Formation *of hydroxyapatite at low supersaturation.* J. Phys. Chem., **80**, 40-45.

ChAng P.L. and prince C.W. (1991) - *1α, 25-Dihydroxyvitamin D_3 stimulates synthesis and secretion of nonphosphorylated osteopontin (secreted phosphoprotein 1) in mouse JB& epidermal cells.* Cancer Res., **51**, 2144-2150.

Cheng P. (1987) - *Formation of octacalcium phosphate and subsequent transformation to hydroxyapatite at low supersaturation: a model for cartilage calcification.* Calcif. Tissue Int., **40**, 339-343.

crAig A.M. and denhArdt D.T. (1991) - *The murine gene encoding secreted phosphoprotein 1 (osteopontin): Promoter structure, activity, and induction in vivo by estrogen and progesterone.* Gene, **100**, 163-171.

curry N.A. and jones D.W. (1971) - *Crystal structure of brushite, calcium hydrogen ortophosphate dihydrate: a neutron-diffraction investigation.* J. Chem. Soc. (A), 3725-3729.

de groot K., geesinK r., klein C.P.A.T. and sereKiAn P. (1987) - *Plasma sprayed coatings of hydroxylapatite.* J. Biomed. Mater. Res., **21**, 1375-1381.

denhArdt D.T. and guo X. (1993) - *Osteopontin: a protein with diverse functions.* The FASEB J., **7**, 1475-1482.

elliot J.C., MAcKie P.E. and young R.A. (1973) - *Monoclinic hydroxyapatite.* Science, **180**, 1055-1057.

fulMer M.T. and brown P.W. (1998) - *Hydrolysis of dicalcium phosphate dihydrate to hydroxyapatite.* J. Mater. Sci. - Mater. Med., **9**, 197-202.

gAdAletA s.g., pAschAlis e.p., betts f., Mendelsohn R. and bosKey A.L. (1996) - *Fourier Transform Infrared Spectroscopy of the Solution-Mediated Conversion of amorphous Calcium Phosphate to Hydroxyapatite: New Correlations between X-ray Diffraction and Infrared Data.* Calcif. Tissue Int., **58**, 9-16.

grAhAM S. and brown P.W. (1996) - *Reactions of octacalcium phosphate to form hydroxyapatite.* J. Cryst. Growth, **165**, 106-115.

grAses f., söhnel o., vilAcAMpA A.I. and MArch J.G. (1996) - *Phosphates precipitating from artificial urine and fine structure of phosphate renal calculi.* Clin. Chim. Acta, **244**, 45-67.

hing K.A., best S.M., tAnner K.E., bonfield W. and revell P.A. (1997) - *Biomechanical assessment of bone ingrowth in porous hydroxyapatite.* J. Mater. Sci. - Mater. Med., **8**, 731-736.

hoyer J.R. (1994) - *Uropontin in urinary calcium stone formation.* Min. Electrolyte Metab., **20**, 385-392.

hunter G.K., hAuschKA P.V., poole A.R., rosenberg L.C. and goldeberg H.A. (1996) - *Nucleation*

and inhibition of hydroxyapatite formation by mineralized tissue proteins. Bioch. J., **317**, 59-64.

Iijima M., Kamemizu H., Wakamatsu N., Goto T., Doi Y. and Moriwaki Y. (1997) - *Transition of octacalcium phosphate to hydroxyapatite in solution at pH 7.4 and 37 °C.* J. Cryst. Growth, **181**, 70-78.

Iijima M., Nelson d.g.A., pan y., Kreinbrink A.t., Adachi M., Goto T. and Moriwaki Y. (1996) - *Fluoride Analysis of Apatite Crystals with a Central Planar OCP Inclusion: Concerning the Role of F^- Ions on Apatite/OCP/Apatite Structure Formation.* Calcif. Tissue Int., **59**, 377-384.

Jarcho M., bolen c.h., thomas M.b., bobick J., Kay R.H. and doremus R.H. (1976) - *Hidroxylapatite synthesis and characterization in dense polycrystalline form.* J. Mater. Sci., **11**, 2027-2035.

Kandori K., yasukawa A. and ishikawa T. (1995) - *Preparation and characterization of spherical calcium hydroxyapatite.* Chem. Mater., **7**, 26-32.

Kay M.i., young R.A. and posner A.S. (1964) - *Crystal structure of hydroxyapatite.* Nature, **204**, 1050-1052.

Lazić S. (1995) - *Microcrystalline hydroxyapatite formation from alkaline solutions.* J. Cryst. Growth, **147**, 147-154.

lemons J.E. (1988) - *Hydroxyapatite coatings.* Clin. Orthop. Relat. Res., **235**, 220-223.

liu D.M. (1995) - *Fabrication and characterization of porous hydroxyapatite granules.* Biomaterials, **17**, 1955-1957.

luo P. and nieh T.G. (1996) - *Preparing hydroxyapatite powders with controlled morphology.* Biomaterials, **17**, 1959-1964.

Mathew M., brown w.e., schroeder L.W. and dickens B. (1988) - *Crystal structure of octacalcium bis(hydrogenphosphate) tetrakis(phosphate) pentahydrate, $Ca_8(HPO_4)_2(PO_4)_4(H_2O)_5$.* J. Crystallogr. Spectrosc. Res., **18(3)**, 235-250.

Mazzè R. (2000) - *Compositional – structural heterogeneity of phosphatic remains. Implications and potential correlations with phases produced in synthesis.* Plinius, **23**, 108 – 112.

Mazzè R. (2002 a) - *Studio strutturale ecomposizionale di bioreperti umani provenienti dalla Valle del Nilo.* Plinius, **28**, 206-208.

Mazzè R. (2002 b) - *Azione inibitrice svolta dalla proteina acida osteopontina sulla nucleazione e crescita di cristalli di idrossiapatite.* Plinius, **28**, 202-204.

Mazzè R. (2002 c) - *Produzione in sintesi di idrossiapatite da soluzioni a pH controllato con tecniche a diffusione di vapore.* Plinius, **28**, 204-206.

Mazzè R. (2003 a) - *Metodi geochimico – mineralogici per valutare la misura dell'alterazione della frazione apatitico – inorganica di bioreperti di vertebrati*. In: GEOITALIA, 4° F.I.S.T., 418-419.

Mazzè R. (2003 b)- *Produzione in sintesi in sistemi controllati di cristalli singoli di calcite e struvite come fasi antagoniste dell'idrossiapatite.* In: GEOITALIA, 4° F.I.S.T., 641-643.

Mazzè R. and degAnello S. (2000) - *Accrescimento di idrossiapatite per diffusione di vapore.* Plinius, **24**, 138-140.

McKee M.D. and nanci A. (1996) - *Osteopontin at mineralized tissue interfaces in bone, teeth, and osseointegration implants: ultrastructural distribution and implications for mineralized tissue formation, turnover, and repair.* Microsc. Res., **33**, 141-164.

McKee M.d., nanci A. and khan S.R. (1995) - *Ultrastructural immunodetection of osteopontin and osteocalcin as major matrix components of renal calculi.* J. Bone Min. Res., **10**, 1913-1929.

Min w., shirag h., chaiko c., goldfarb s., krishna G.G. and hoyer J.R. (1998) - *Quantitative studies of human urinary excretion of uropontin.* Kidney Int., **53**, 189-193.

Monma H. and kamiya T. (1987) - *Preparation of hydroxyapatite by the hydrolysis of brushite.* J. Mater. Sci., **22**, 4247-4250.

Montel g., bonel g., heughebaert J.c., trombe J.C. and rey C. (1981) - *New concepts in the composition, crystallization and growth of the mineral component of calcified tissues.* J. Cryst. Growth, **53**, 74-99.

nelson D.G.A. and featherstone J.D.B. (1982) - *Preparation, analysis, and characterization of carbonated apatites.* Calcif. Tissue Int., **34**, S69-S81.

nelson D.G.A. and mclean J.D. (1984) - *High - resolution electron microscopy of octacalcium phosphate and its hydrolysis products.* Calcif. Tissue Int., **36**, 219-232.

newesely H. (1989) - *Fossil bone apatite.* Appl. Geochem., **4**, 233-245.

noda M., vogel r.l., craig A.M., prahl J., de luca H.F. and denhardt D.T. (1990) - *Identification of a DNA sequence responsible for binding of the 1,25-Dihydroxyvitamin D_3 receptor and 1,25-Dihydroxyvitamin D_3 enhancement of mouse secreted phosphoprotein 1(Spp-I or osteopontin) gene expression.* Proc. Nat. Acad. Sci. U.S.A., **87**, 9995-9999.

nonAMi t., KAMiyA A., nAgAnuMA K. and KAMeyAMA T. (1998) - *Preparation ofhydroxyapatite-granule implanted superplastic titanium-alloy*. J. Mater. Sci. - Mater. Med., **9**, 203-206.

piepenbrinK H. (1989) - *Examples of chemical changes during fossilization*. Appl. Geochem., **4**, 273-280.

pouchou J.L. (1984) - *A new model for x-ray microanalysis.* Rech. Aérosp., **3**, 167-192.

reinholt f.p., hultenby K., oldberg A. and heinegård D. (1990) - *Osteopontin – a possible anchor of osteoclasts to bone*. Proc. Nat. Acad. Sci. U.S.A., **87**, 4473-4475.

sAntos M. and gonzá1ez-díAz P.F. (1980) - *Ultrastructural study of apatites in human urinary calculi*. Calcif. Tissue Int., **31**, 93-108.

sudA h., yAshiMA M., KAKihAnA M. and yoshiMurA M. (1995) - *Monoclinic ↔ hexagonal phase transition in hydroxyapatite studied by x-ray powder diffraction and differential scanning calorimeter techniques.* J. Phys. Chem., **99**, 6752-6754.

sudArsAnAn K. and young R.A. (1969) - *Significant precision in crystal structural details: Holly Springs hydroxyapatite*. Acta Cryst., **B25**, 1534-1543.

tAnAhAshi M., KoKubo t., nAKAMurA t., KAtsurA Y. and nAgAno M. (1996) - *Ultrastructural study of an apatite layer formed by a biomimetic process and its bonding to bone*. Biomaterials, **17**, 47-51.

wAng c.K., chern lin J.h., Ju c.p., ong H.C. and ChAng R.P.H. (1997) - *Structural characterization of pulsed laser-deposited hydroxyapatite film on titanium substrate*. Biomaterials, **18**, 1331-1338.

yoon K., buenAgA R. and rodAn R.A. (1987) - *Tissue specifity and development expression of rat osteopontin*. Biochem. Biophys. Res. Commun., **148**, 1129-1136.

young R.A. and hoIcoMb D.W. (1982) - *Variability of hydroxyapatite preparations.* Calcif. Tissue Int., **34**, S17-S32.